

Evaluation of correction methods for errors in T₂* quantification caused by background gradients

Ruitian Song¹, Travis Bevington¹, Brian A Taylor¹, Axel J Krafft¹, Ralf B Loeffler¹, and Claudia M Hillenbrand¹
¹Radiological Sciences, St Jude Children's Research Hospital, Memphis, Tennessee, United States

Introduction: Accurate measurement of T₂* is of importance for many basic, preclinical, and clinical MR applications. Examples include blood oxygenation level dependent functional (BOLD) imaging [1], super-paramagnetic iron oxide contrast imaging [2], and tissue iron quantification in the brain [3], heart [4], and liver [5]. However, T₂*-measurement accuracy can be influenced by macroscopic field inhomogeneities (i.e., background gradients) that are introduced by susceptibility changes, e.g. at air-tissue boundaries. Two major approaches have been proposed to correct for the errors in T₂*-quantification that arise from background gradients: (a) *sinc*-weighted fitting of the signal decay (FIT) [6], and (b) direct measurement of the field ΔB₀ (DMF) [7]. As no formal comparison of both strategies has been performed yet, the pros and cons associated with each technique are unclear as well as which technique should be used for a certain application. Purpose of this work is to compare and evaluate these two methods in phantoms and *in vivo* with specific focus on hepatic imaging.

Materials and Methods: The MR signal M acquired by a multi-echo spoiled gradient echo (mGRE) sequence can be expressed as: $M(TE) = d \cdot M_0 \cdot \exp(-TE/T_2^*) \cdot \text{sinc}(\gamma TE G_b d/2)$ [Eq.1] where TE is the echo time, d the slice thickness, and G_b the background gradient caused by field inhomogeneities. When using FIT, G_b is treated as an unknown parameter and T₂* is obtained by a three parameter fit (T₂*, M₀, and G_b) [6]. For DMF, G_b is estimated from B₀ field maps calculated by phase images obtained from the mGRE acquisition; after G_b has been determined, T₂* is calculated by a two parameter fit (T₂* and M₀) [7]. The gradient calculation relies on the field information of two neighboring slices. Therefore, no gradient can be determined for the two outmost slices of an image stack [7]. In this study, Autoregressing Moving Average Modeling (ARMA) [8] is used to generate field maps and the resulting G_b maps. All algorithms were implemented in Matlab (MathWorks), and fitting was performed on a voxel-by-voxel basis. **Phantom Scans:** to generate field inhomogeneities caused by air/water boundaries, an empty cuboid bottle (volume 7.5×7.5×18cm³) was sealed and glued into a square container (volume 20×20×19cm³) filled with 8.33mM Gd-doped water (Fig. 1). Images were acquired on a 1.5T scanner (Siemens Avanto) using an mGRE sequence with 20 echoes. Parameters were as follows: TE_{min} 0.98ms, echo spacing 1.38ms, TR 200ms, flip angle 25°, FOV 24×30cm, and matrix size 128×104. Seven coronal slices were acquired with a slice thickness and inter slice gap of 10mm. **In Vivo Scans:** hepatic imaging of healthy volunteers was performed on a 3T scanner (Siemens Trio) using the mGRE sequence with 20 echoes in a single breathhold. Acquisition parameters were TE_{min} 1.73ms, echo spacing 1.29ms, TR 200ms, flip angle 35°, FOV 28.4×35cm, and matrix size 128×104. Nine transverse slices were acquired, starting from the diaphragm and covering the liver with a slice thickness of 10mm and no gap. Only the 7 center slices were used for the calculations.

Results and Discussion: Table 1 summarizes the results obtained for the phantom at specific locations ROI 1 & 2 (Fig. 2) and a healthy volunteer (male, age 23y). **Phantom Scans:** The effect of background gradients was not observed when the ROI was far away from the air/water boundary. In that case (slices 1 & 2 for ROI 1 and slices 1-4 for ROI 2) the uncorrected T₂* values were around 20ms. For slice 1, uncorrected and FIT T₂* values are very close. Approaching the air/water boundary, uncorrected T₂* values decreased (bold), indicating that increasingly stronger background gradients impact the decay. FIT-corrected T₂* values were around 20ms (range 18.2-20.7ms) for both ROIs. This indicates that the FIT correction works properly. The DMF algorithm corrected slice 2 pretty well, but showed over-correction for both ROIs for slice indices approaching the air/water boundary. Slice 7 was placed too close to the empty bottle, so that no T₂* map could be calculated with either approach. **In Vivo:** The last column of Table 1 shows the results obtained for a healthy volunteer. Here, the first slice is close to the lung/liver interface. Steep drops in uncorrected T₂* can be seen for the first few slices (bold) because of background gradients caused by the lung/liver boundary. At the center of the liver (slice 7, portal vein level), the uncorrected liver T₂* reaches a maximum of 20.3ms. As this is a healthy volunteer, the T₂* of liver tissue should not vary strongly within the organ. It therefore seems reasonable to attribute the observed deviation of approximately 50% in liver T₂* between slices 1 & 2 and slice 7 to stronger background gradients near the lung/air interface. FIT recovered T₂* to approx. 24–25ms. However, for slice 1 the value could still not be completely corrected. DMF corrected slices 5-7 in the center of the liver well where background gradients are small. However, the DMF correction seemed to deteriorate the closer a slice gets to the lung/liver interface.

Conclusion: There is a need for correction of T₂* values in areas of strong susceptibility changes. By comparing FIT and DMF, we found that FIT worked better in correcting T₂*. DMF is not very accurate and prone to over- or underestimation. The reason is that the field maps (and the resulting gradient) calculated from phase images represent the magnitude of all three (x,y,z) field components. However, G_b in Eq.[1] is only the gradient component along the z direction. This can cause over- or undercorrection of T₂*. Our results indicate, that FIT is preferred unless the z component of the magnetic field dominates among the three spatial components.

References: [1] Sadowski EA et al. MRI 2010;28:56-64. [2] Dahnke H et al. MRM 2005;53:1202-6. [3] Gelman N et al. Radiology 1999;210:759-67. [4] Hankins J et al. Ped Blood&Cancer 2010;55:495-500. [5] Hankins J et al. Blood 2009;113:4853-5 [6] Fernandez-Seara M et al. MRM 2000;44:358-66. [7] Hernando D et al. MRM 2012;68:830-40. [8] Taylor BA et al. JMIR 2012;35:1125-32.

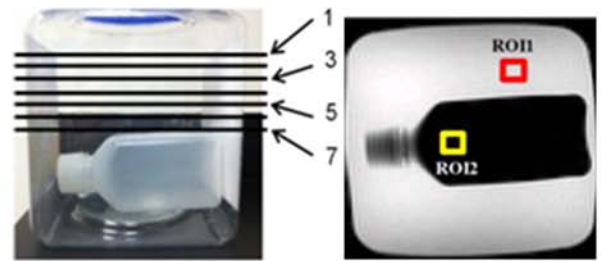


Fig 1. Phantom with slice positions.

Fig 2. ROI locations.

Table 1. Summary of T₂* corrections for the phantom and a volunteer

slice	ROI 1 T ₂ * [ms]			ROI 2 T ₂ * [ms]			Volunteer T ₂ * [ms]		
	Uncorr	FIT	DMF	Uncorr	FIT	DMF	Uncorr	FIT	DMF
1	20.0	20.5	--	20.1	20.5	--	9.9	16.9	10.5
2	19.4	20.2	22.5	20.4	20.6	20.8	9.3	22.5	13.6
3	18.8	20.2	26.6	20.4	20.8	20.5	12.5	24.9	16.5
4	16.9	20.0	90.9	20.2	20.7	23.5	14.0	25.8	17.0
5	11.6	18.4	32.7	14.5	19.1	70.0	17.5	24.4	20.1
6	15.0	19.3	--	9.9	18.2	--	18.3	25.3	20.1
7	--	--	--	--	--	--	20.3	28.4	20.7